*International Journal of Research in Engineering and Science (IJRES)*
*ISSN (Online): 2320-9364, ISSN (Print): 2320-9356*
*www.ijres.org Volume 10 Issue 7 ǁ July 2022 ǁ PP. 816-828*

# Modelling of Wide range output DC-DC converter for EV Charging

Syamily K V*[1],Chaithanya P R[1] ,Govindraman S[1],Illyas Muhammad Arjuvan[1], Prof.Elizabeth Paul[1]

[1]*Mar Athanasius College of Engineering , Kothamangalam ,Kerala, India*
*Corresponding Author:*syamilykv243@gmail.com*

***Abstract***
*Nowadays the charging infrastructure of electric vehicles becomes very important as the EV market grows. There are two main charging connector protocols available. They are Charge de Move (CHAdeMO) which covers a low voltage battery range up to 500V, and combined charging system (CCS), covers a relatively high voltage battery up to 950V. In order to be compatible with all EVs adapting either CHAdeMO or CCS, it is necessary to develop a universal EV charger that covers an extremely wide range of the battery voltage. A Pulse Width Modulation (PWM) controlled Series Resonant Converter (SRC) is introduced for the development of a universal charger and it is focussed on the boost mode of SRC. By adjusting two PWM boost switches with a full bridge rectifier, it is viable for a SRC to cover a very wide range of gain with a high and flat efficiency curve. As the output voltage increases, the secondary side rectifier of the SRC gradually changes from a full bridge rectifier to a voltage doubler rectifier. When the switching frequency is fixed to the resonant frequency in boost mode, the converter achieves "two peak efficiency points" with full bridge and voltage doubler rectifiers. The efficiency drop over the wide range of gain is controlled by these two peak efficiency points, and this is the reason why the proposed converter achieves a high and flat efficiency curve.*

***Keywords:*** *Series resonant converter, pulse width modulation, electric vehicle, electric vehicle charger, universal charger.*

---

Date of Submission: 14-07-2022 Date of acceptance: 28-07-2022

---

## I. INTRODUCTION

Over the past decade, electric vehicles (EVs) have become one of the primary technologies to assist society in achieving ambitious clean energy and decarbonization goals.Two main charging connector protocols exist are CHAdeMO and CCS, and they have different ranges of battery voltage. By combining the features of these two, it is possible to develop a universal charger that is compatible for the different battery ranges. The DC/DC converter for the universal charger needs to achieve high efficiency over the entire output voltage range.Due to soft switching and a small number of components, series resonant converter (SRC) and LLC converter have been widely used in various applications. Both of these converters are similar to each other in that they utilize series-connected resonant inductor and capacitor as the main resonant components. The main difference between SRC and LLC converter is the magnetizing inductance value of the transformer. SRC has a large magnetizing inductance of the transformer, whereas LLC has a small value. Circulating loss due to large magnetizing inductance in SRC is small, resulting in a higher efficiency at the resonant frequency. However, SRC provides only step down voltage conversion ratio, whereas LLC converter achieves a high gain when the switching frequency becomes smaller. This is because the circulating current which is stored in the resonant capacitor and the energy is delivered to the output side in the next switching period. From these, it can be noticed that SRC has a smaller circulating current but also a limited range of the gain. Therefore, if a wider range of gain can be achieved in SRC, it would be possible to have both a small circulating current and a wide range of gain.

Generally, resonant converters operate with variable switching-frequency control. When operating above the resonant frequency, a resonant converter operates with zero- voltage switching (ZVS) of the primary switches. Generally, variable switching-frequency control is seen as a drawback of a resonant converter especially in applications with a wide input voltage and/or output voltage range. Specifically, as the input or output voltage range increases, the control frequency range also increases so that driving and magnetic component losses also increase, thereby reducing conversion efficiency. There are several approaches to provide SRC a wider range of gain. One of the best approach is pulse width modulation (PWM) adapted resonant converters. In this, PWM signals create a boosting period which boosts the resonant current so that a resonant

converter can achieve boosting gain. By doing so, a wide range of voltage conversion ratio can be covered with a narrower switching frequency range. The main concern is a large peak of the resonant current when a high boosting gain is required. This large peak of the resonant current causes large rms current and turnoff loss from the boosting switches. Topology-morphing technique is the second approach. In this, a certain switching component is controlled to reconfigure inverter or rectifier structure. By doing so, the gain can be deducted by half and the converter can achieve a wide range of gain with full bridge and half bridge inverter operation. Because an abrupt change in the configuration of the converter can cause output voltage dip and swell, a solution for smooth transition between full bridge and half bridge configuration is investigated.

A PWM controlled SRC for a universal EV charger that requires an extremely wide range of gain. This work mainly focuses on the boost mode of a SRC. As the output voltage increases, the secondary side rectifier of the proposed converter gradually converts from a full bridge rectifier to a voltage dou- bler rectifier with a simple PWM control. Since the switching frequency is fixed to the resonant frequency in boost mode, the proposed converter naturally achieves "two peak efficiency points" with full bridge and voltage doubler rectifiers. Since two peak efficiency points limit the efficiency drop over a wide range of gain, the proposed converter achieves a high and flat efficiency curve.

## II. CHARGING PROTOCOLS

Electric vehicle charging infrastructure becomes more im- portant as the EV market grows. There are mainly two mainstreams of charging connector protocols that exist for EV charging. They are Charge de Move (CHAdeMO) and com- bined charging system (CCS), and they have different ranges of battery voltage. Usually, CHAdeMO covers a relatively low voltage battery range and CCS covers a relatively high voltage battery range.

### (i) CHAdeMO

CHAdeMO(charge de move) is a DC charging standard for electric vehicles. It enables seamless communication between the car and the charger. It is a rapid charging standard, meaning it can supply a vehicle's battery with capacity batteries can be charged in a relatively short period of time. It is one of a selection of rapid charging standards which was created by a consortium of carmakers and industry bodies that now includes more than 400 members and 50 charging companies. Its name stands for Charge de Move, which is also the name of the consortium. The goal of the consortium was to develop a fast-charging vehicle standard that the whole automotive industry could adopt.

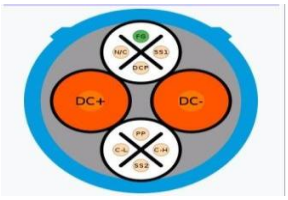


**Figure 1: CHArge de MOve (CHAdeMO) .**

### (ii) Combined Charging System

The Combined Charging System (CCS) is a standard for charging electric vehicles, which uses the Combo 1 and Combo 2 connectors to provide power at up to 350 kilowatts. These two connectors are extensions of the IEC 62196 Type 1 and Type 2 connectors, with two additional direct current (DC) contacts to allow high-power DC fast charging.CCS charging is only for DC rapid charging of 50kW or more. The two larger, lower pins on the plug enable the Direct Current connection that forces more electricity into your batteries in less time. It gets the "combined" part of its name as the connector builds on a low-power, slow-charging Type 2 connector. The CCS connector uses some connections of the Type 2 interface and adds two additional DC power lines which are capable of running at higher voltages compared to the standard connector.

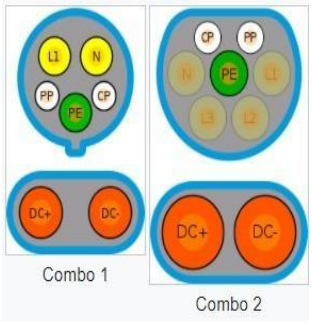


**Figure 2: Flow chart of P&O algorithm**

## III. SERIES RESONANT CONVERTER

In order to develop a universal charger which covers voltage levels of both CHAdeMO and CCS,the DC/DC converter needs to achieve a high efficiency over the entire output voltage level. This high efficiency points is achieved by adapting two PWM boost switches with a full bridge rectifier. And thereby presents a PWM controlled series resonant converter for a universal EV charger that requires an extremely wide range of gain.The converter has an input voltage source provided with an input voltage VIN, and it consists of half bridge switches QPA1 and QPA2, resonant inductor LR, resonant capacitor CR, and a transformer with the turns ratio NP:NS = n:1 in its primary side. The secondary side rectifier of the proposed converter is a full bridge rectifier, but it also commits two switches QSR1 and QSR2, a blocking capacitor CB. QPA1 and QPA2 are driven with complementary signals with 0.5 duty cycle.

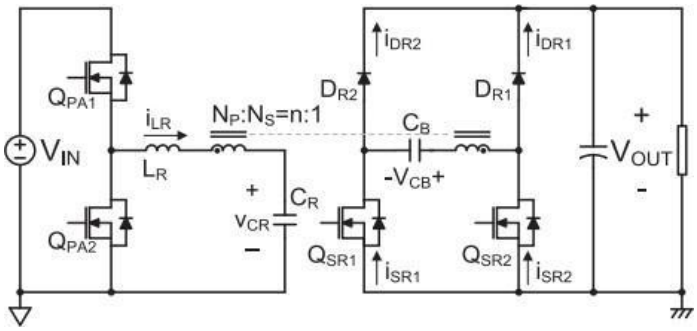


**Figure 3: Series Resonant Converter**

## IV. MODES OF OPERATION

The boost region is having two regions;PWM 1 & PWM 2. Switching frequency of boost region is close to fR in order to have maximum gain and minimize circulating current in SRC.

### (i) CONVENTIONAL FREQUENCY MODULATION

Initially, the proposed converter is controlled by conven- tional frequency modulation. In this mode, the converter is in the buck region. Here QPA1 and QPA2 are driven with complementary signals with 0.5 duty cycle. The switching frequency increases as VOUT decreases.

### 1.1.1 PWM1

PWM 1 focuses on the boost region where the switching frequency is close to fR. When VOUT = VIN/2n, the proposed converter operates as a conventional half bridge SRC with full bridge rectifier. When VOUT is between VIN/2n and VIN/n, secondary side rectifier operates as a full bridge rectifier with a boosting duty cycle DB.

**1.1 Mode 1 [t0–t1]:**

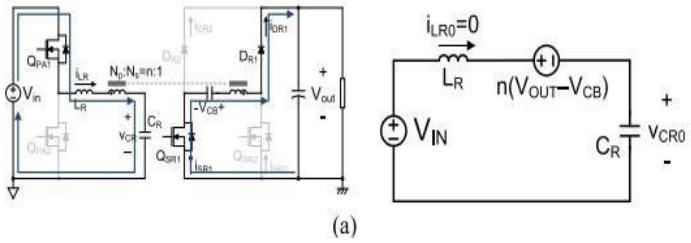


**Figure 4: Current paths and equivalent resonant circuit during mode1**

Mode 1 begins as QPA1 is turned ON. The resonant inductor current at t0(iLR0) is zero. Resonant components LR and CR resonate and the resonant current is delivered to the output capacitor through transformer and secondary side rectifier components DR1 and QSR1. QSR1 is turned ON as a synchronous rectifier. Mode 1 lasts for the half resonant period. Thus, iLR becomes zero again at the end of Mode 1 and it ends when QPA1 is turned OFF.

$Zi_{LR}(t)= [V_{IN} - n(V_{OUT}- V_{CB}) - v_{CRO}]\sin(\omega t)$ (1)

$v_{CR}(t) - V_{IN}+ n(V_{OUT} - V_{CB})=-[V_{IN}- n(V_{OUT} - V_{CB}) - v_{CRO}]\cos(\omega t)]$ (2)

$[v_{CR}(t) - V_{IN}+ n(V_{OUT} - V_{CB}]^2+ [Zi_{LR}(t)]^2= [V_{IN} - n(V_{OUT} - V_{CB}) - v_{CRO}]^2= R^2$(3)

**1.2 Mode [t1–t2]:**

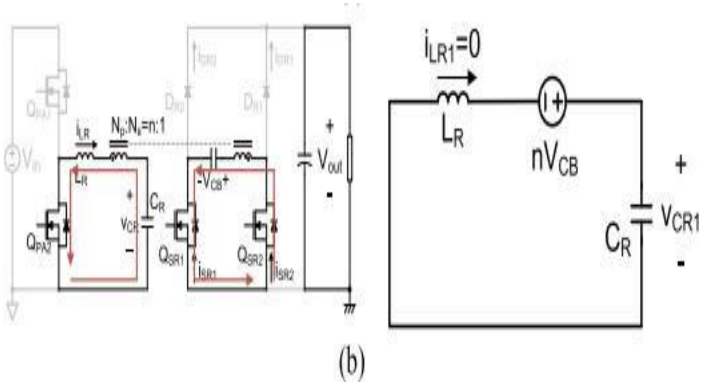


**Figure 5: Current paths and equivalent resonant circuit during mode2**

Mode 2 begins as QPA2 is turned ON. iLR1 is zero as before. QSR1 is still turned ON due to extended duty cycle, hence iLR is boosted fast. This mode provides a boosting capability of the proposed converter. QSR1 is turned OFF after iLR is boosted enough, and Mode 2 ends.

$Zi_{LR}(t) = [n(V_{CB} - v_{CR1}]\sin[\omega(t - t_1)]$ (4)

$v_{CR}(t) - nV_{CB}= -[nV_{CB} - v_{CR1}]\cos[\omega(t - t1)]$ (5)

$[v_{CR}(t)-nV_{CB}] +[Zi_{LR}(t)] = [nV_{CB}-v_{CR1}] = R.$ (6)

**1.3 Mode 3 [t2–t3]:**

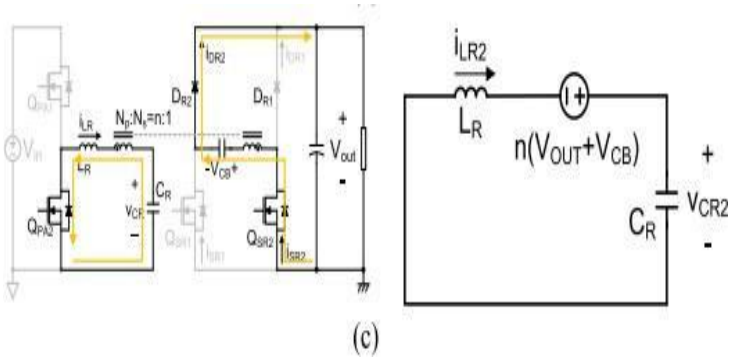


**Figure 6: Current paths and equivalent resonant circuit during mode3**

Mode 3 begins when the rectifier diode DR2 and QSR2 are turned ON. Boosted resonant current in Mode 2 is delivered to the output side, and iLR decreases. Mode 3 lasts till iLR reaches zero and DR2 and QSR2 are turned OFF.

During the remainder switching period (mode 4), small mag- netizing current of the transformer freewheels through QPA2.
To avoid complexity, the current during mode 4 is assumed to be zero in state analysis. When QPA2 is turned OFF and QPA1 is turned ON at t = TS, the proposed converter goes back to mode 1.

$$Zi_{LR}(t) = Zi_{LR2}\cos[\omega(t - t_2)]+[n(V_{OUT} + V_{CB}) - v_{CR2}]\sin[\omega(t - t_2)] \quad (7)$$

$$v_{CR}(t) - n(V_{OUT} + V_{CB}) = Zi_{LR2}\sin[\omega(t - t_2)] -[n(V_{OUT} + V_{CB}) - v_{CR2}]\cos[\omega(t - t_2)] \quad (8)$$

$$[v_{CR}(t) - n(V_{OUT} + V_{CB})]^2 + [Zi_{LR}(t)]^2=[Zi_{LR2}]^2 + [n(V_{OUT} + V_{CB}) - v_{CR2}]^2 = R^2 \quad (9)$$

**1.2.1 PWM2**

The converter enter PWM2 region when voltage higher than VIN/n is needed.So the duty cycle DB is need to be larger than 0.5. In PWM 2 region QSR1 is completely turned ON. When VOUT become equal to VIN/n,the secondary side rectifier of the proposed converter is gradually converted from a full bridge rectifier to a voltage doubler rectifier as DB becomes 0.5.
Operation in PWM 2 region is quite similar with that of PWM 1, state equations in each three mode can be obtained.

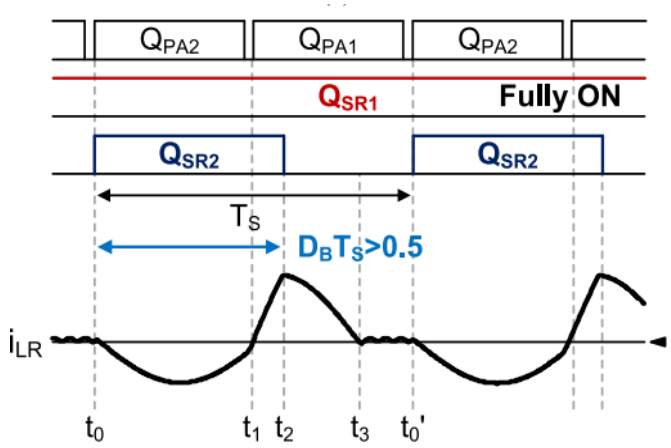


**Figure 7: Simulink Model of Grid Tied Inverter**

**1.1 Mode 1 [t0–t1]:**

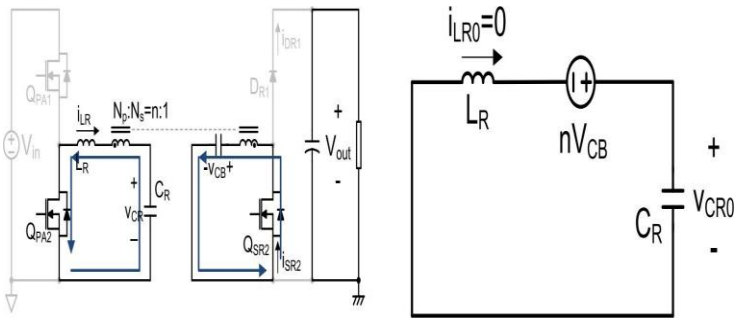


**Figure 8:Current paths and equivalent resonant circuit during mode1**

Mode 1 begins as QPA2 is turned ON. The resonant inductor current at t0(iLR0) is zero. Resonant components LR and CR resonate and the resonant current is delivered to the output capacitor through transformer and secondary side rectifier components QSR1 and QSR2. QSR2 is turned ON as a synchronous rectifier. Thus, iLR becomes zero again at the end of Mode 1 and it ends when QPA2 is turned OFF.

$Zi_{LR}(t) = [nV_{CB} - v_{CRO}]\sin(\omega t)$ (10)

$v_{CR}(t) - nV_{CB} = -[nV_{CB} - v_{CRO}]\cos(\omega t)$ (11)

$[v_{CR}(t) - nV_{CB}]^2 + [Zi_{LR}(t)]^2 = [nV_{CB} - v_{CRO}]^2 = R_1^2$

**1.2 Mode 2 [t1-t2]:**

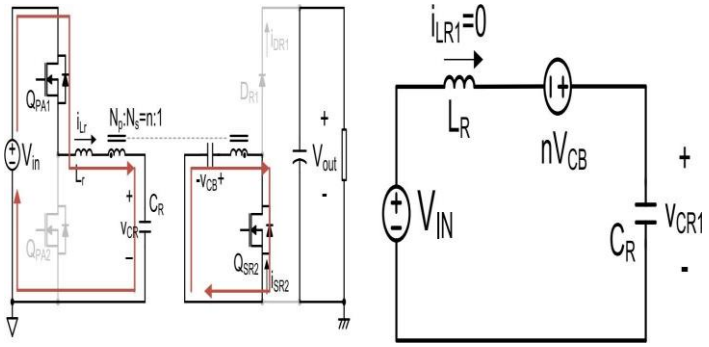


**Figure 9: Current paths and equivalent resonant circuit during mode2**

Mode 2 begins as QPA1 is turned ON. iLR1 is zero as before. QSR2 is still turned ON due to extended duty cycle, hence iLR is boosted fast. This mode provides a boosting capability of the proposed converter. QSR2 is turned OFF after iLR is boosted enough, and Mode 2 ends.

$Zi_{LR}(t) = [V_{IN} + n(V_{CB} - v_{CR1}]\sin[\omega(t - t_1)]$ (13)

$v_{CR}(t)\ (V_{IN} + nV_{CB}) = [V_{IN} + nV_{CB}\ v_{CR1}]\cos[\omega(t - t_1)]$ (14)

$v_{CR}(t) - (V_{IN} + nV_{CB})]^2 + [Zi_{LR}(t)]^2 = [V_{IN} + nV_{CB} - v_{CR1}]^2 = R_2$ (15)

**1.3 Mode 3 [t2-t3]:**

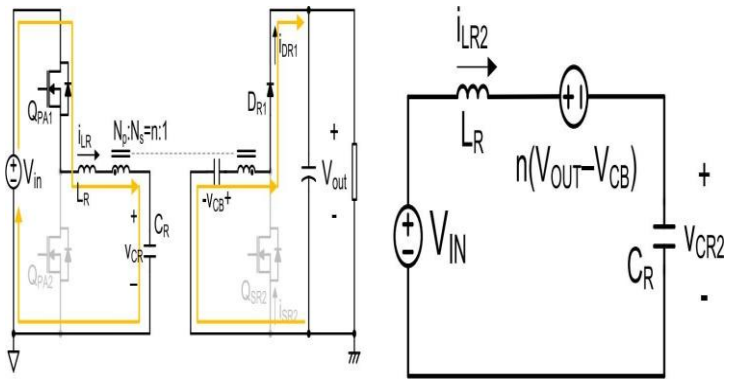


**Figure 10: Current paths and equivalent resonant circuit during mode3**

Mode 3 begins when the rectifier diode DR1 is turned ON. Boosted resonant current in Mode 2 is delivered to the output side, and iLR decreases. Mode 3 lasts till iLR reaches zero and DR1 is turned OFF. During the remainder switching period (mode 4), small magnetizing current of the transformer freewheels through QPA1. To avoid complexity, the current during mode 4 is assumed to be zero in state analysis. When QPA1 is turned OFF and QPA2 is turned ON at t = TS, the proposed converter goes back to mode 1.

$$Zi_{LR}(t) = Zi_{LR2}\cos[\omega(t - t_2)]+[V_{IN} + n(V_{CB} - V_{OUT}) - v_{CR2}]\sin[\omega(t - t_2)] \quad (16)$$

$$v_{CR}(t) - [V_{IN}+ n(V_{CB} - V_{OUT}) = Zi_{LR2}\sin[\omega(t - t_2)]-[V_{IN} + n(V_{CB} - V_{OUT}) - v_{CR2}]\cos[\omega(t - t_2)] \quad (17)$$

$$[v_{CR}(t) - (V_{IN} + n(V_{CB}- V_{OUT}))]2 + [Zi_{LR}(t)]^2=[Zi_{LR2}]^2+ [V_{IN}+ n(V_{CB} - V_{OUT}) - v_{CR2}]^2 = R_2 \quad (18)$$

## V.CONTROL

When the converter works at resonant frequency fR and all switches at the secondary side operate as synchronous rectifiers, the output voltage VOUT becomes VIN/2n.

$$f_R= 1/2\pi\sqrt{L_RC_R} \quad (19)$$

The switching frequency remains at the resonant frequency in the boost region, and the proposed converter has two resonant operating points at VOUT = VIN/2n and VIN/n. Since an SRC shows a highest efficiency with the resonant point operation, the proposed converter can have the two highest efficiency points over a wide gain range.When VOUT =VIN/2n, the switching frequency becomes the resonant frequency, and the proposed converter meets its "first" resonant point with full bridge rectifier. In the boost region, VOUT is controlled by increasing the boosting duty cycle DB. When VOUT is in between VIN/2n and VIN/n, DB varies from 0 to 0.5. The switching frequency remains at the resonant frequency fR and the duty cycle of QSR1 increases. When VOUT = VIN/n, DB becomes 0.5 and QSR1 is fully turned ON and the secondary side rectifier becomes a voltage doubler smoothly, and the proposed converter meets its "second" resonant point with the voltage doubler rectifier. When VOUT = VIN/n, DB is larger than 0.5. The duty cycle of QSR2 increases.

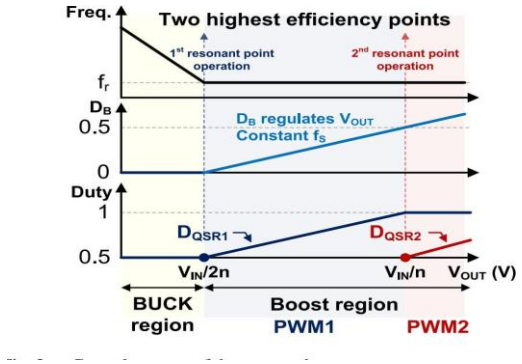


**Figure 11: Control concept**

This represents the efficiency curve with 3.3 kW output condition. Since efficiency drop is limited by two resonant points operation, the efficiency curve can be high and flat around or higher than 98. Although body diodes are used for high side switches. When silicon carbide MOSFETs QSR3 and QSR4 are replaced with silicon carbide diodes, the efficiency would be even closer to that of SR operation, since the forward voltage drop is much smaller in silicon carbide diodes than body diodes.

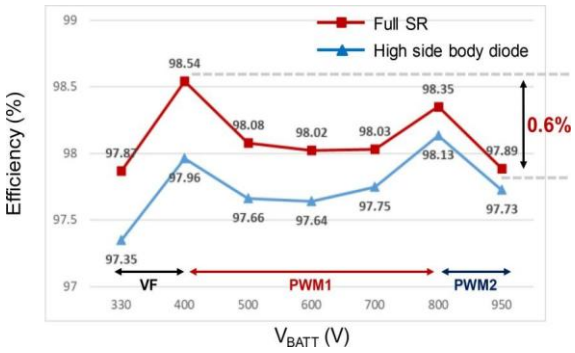


**Figure 12: Two peak efficiency curve**

## VI. SIMULATION

The MATLAB simulation is done to observe the effective- ness of the proposed converter and control has been verified on an 800 V input and 200–950 V/3.3 kW output prototype.

### (i) SIMULATION PARAMETERS

The output waveforms of the prototype converter at 800 V/3.3 kW output condition. QSR1 is fully turned ON, and the converter operates at the second resonant point with a voltage doubler rectifier. The proposed work achieves high efficiency over a very range of output voltage, utilizing a small number of components.

Table 1 shows the simulation parameters of PWM controlled SRC for an input voltage of 800 V and with a switiching frequency of 65 KHz.

| **Parameters** | **Specification** |
|---|---|
| Input Voltage | 800 V |
| Output Voltage | 200- 950 V |
| Switching Frequency | 65 kHz |
| Rated Output Power | 3.3 kW |
| Semiconductor Devices | 6 |

| | |
|---|---|
| Gain Variation | 4.75 |
| Efficiency at full load | 96 - 98% |

**Table 1:Design Specifications For The Series Resonant Converter**

**(ii) SIMULINK MODEL OF SRC**

The PWM Series Resonant Converetr is simulated in MAT- LAB/SIMULINK by choosing the parameters listed in Table 1 and the simulink model is shown in Fig.13.

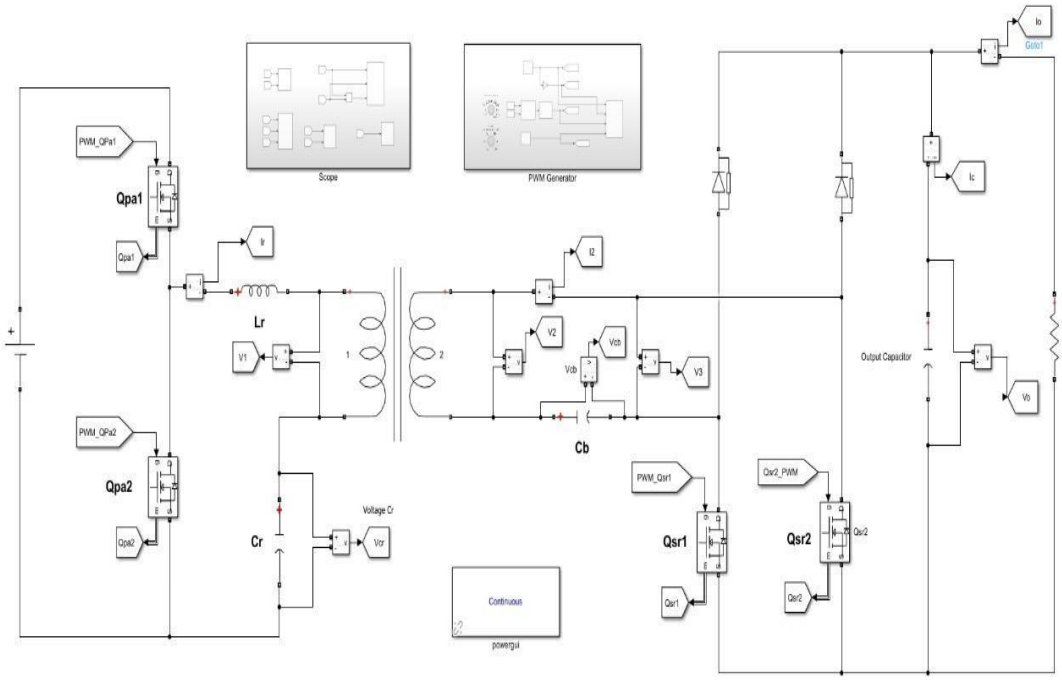


**Figure 13: Simulink model of SRC**

The SRC converter is the primary part of the project. It is incorporated to obtain two peak efficiency points with full bridge and voltage doubler rectifiers. Since two peak efficiency points limit the efficiency drop over a wide range of gain, the proposed converter achieves a high and flat efficiency curve.The input voltage for the converter is of 800 volts dc and the output voltage range is 200 to 950 volts.

**1.1 Subsystem**: **PWM Generator**

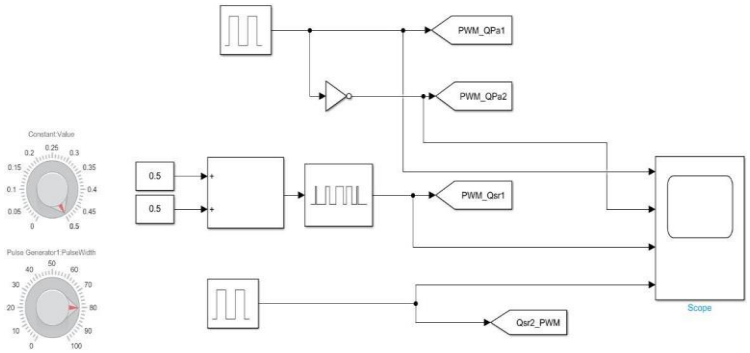


**Figure 14: PWM Genearator**

**1.2 Subsystem: Scopes**

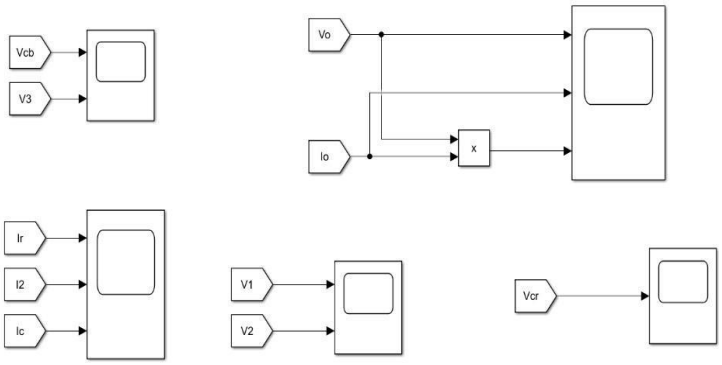


**Figure 15: Various Scopes**

**(iii) SIMULATION RESULTS**

The simulation results of the PWM controlled Series Reso- nant Converter are shown in the following figures. Figure 16 shows the gate pulses to the switches of SRC using two PWM switching.

**1.1 Gate Pulse Generation:-**

In PWM 1 region, the boosting duty cycle DB increases as VOUT increases, with the extended duty cycle of QSR1. When VOUT becomes VIN/n, DB becomes 0.5 and QSR1 is completely turned ON. When VOUT needs to be higher than VIN/n, the proposed converter enters PWM 2 region. DB needs to be larger than 0.5. Since QSR1 is completely turned ON, the duty cycle of QSR2 is extended

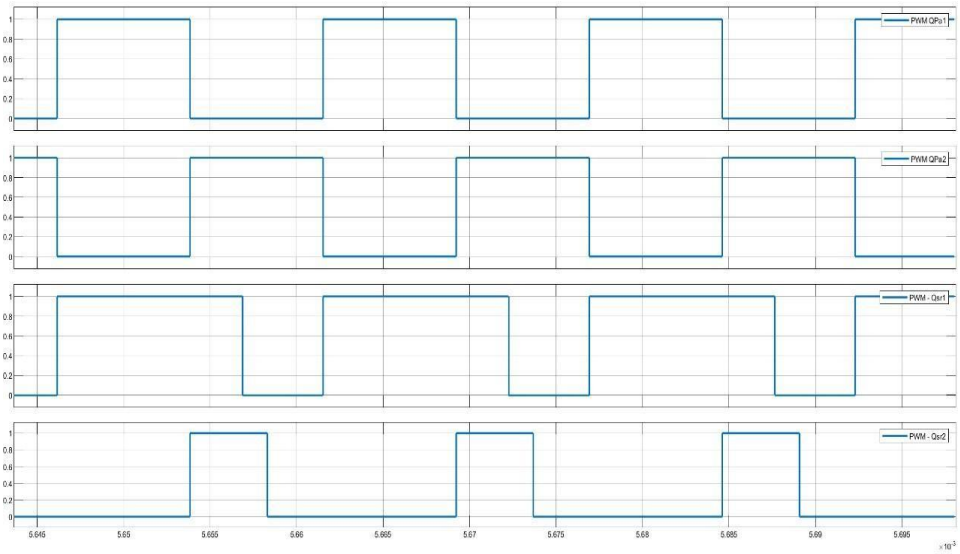


**Figure 16: Generated Pulse**

Fig.17 represents the resonant current waveform with 40 H resonant inductor in PWM 1 region. Since the proposed converter operates the half resonance during the first half of the switching period, two cases have the same positive peak of the resonant current. However, when the resonant current is boosted, it can be noted that the negative peak ILRmax is larger when the resonant inductor is smaller. For these reasons, a large LR value would be preferable if the design pursues a small rms current, small EMI noise, and balanced current tress on devices.

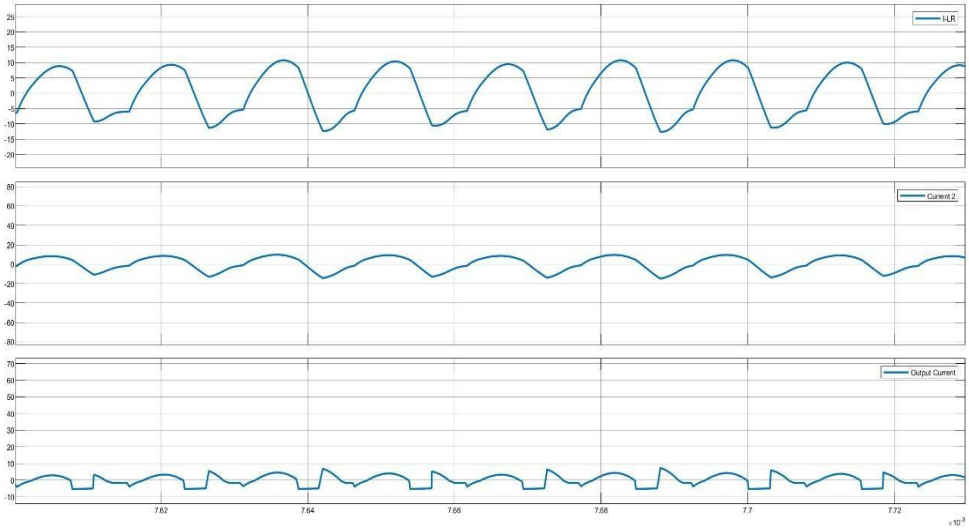


**Figure 17: Resonant current waveform in PWM 1 region**

Fig.18 represents the waveforms of output voltage, current and power in PWM 1 region. In this region, voltage can vary above VIN/2n( ie. VOUT= 400 V). Also current is above 1.5 amperes and get an output power of 800 watts. With a given LM, we can see that ZVS current becomes maximum.when VOUT = 400 and 800 V. This is because the output voltage is applied to the transformer during whole switching period when VOUT = V/2n and VIN/n. In other cases, there is a certain circulating period in a switching cycle.

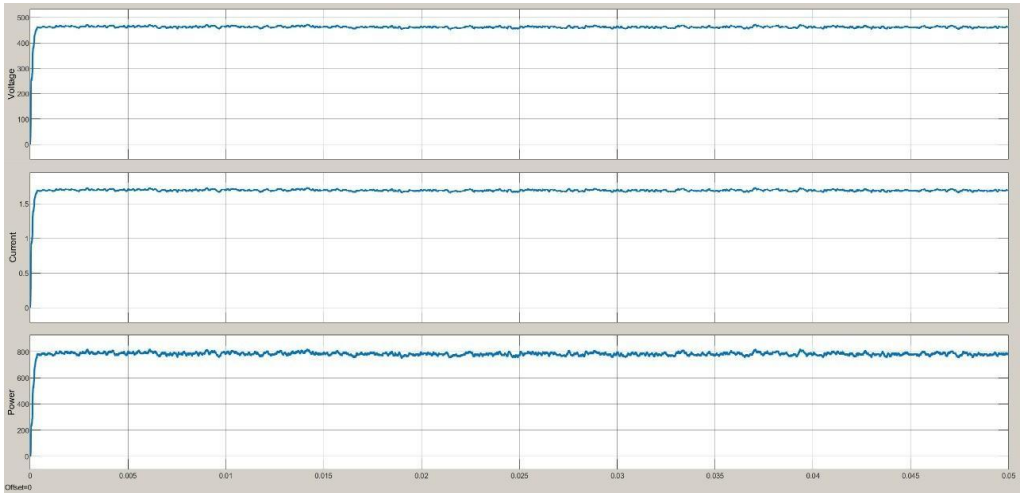


**Figure 18: Output Voltage, Power, Current Level in PWM 1 region**

Fig.19 represents the resonant current waveform of resonant inductor in PWM 2 region. Fig.20 represents the output voltage, current and power in PWM 2 region. Here Voltage is above VIN/n (ie. VOUT=800 V), current is nearly 3.5 amperes and get an output power of 3000 watts. As VOUT increases from 400 V, ILRMAX increase due to boosting period. ILRMAX become maximum when VOUT is around 600 V, and decrease again as VOUT gets close to 800 V, which is the second resonant point with voltage doubler rectifier. Here is the difference between the proposed converter and conventional PWM adapted resonant converter

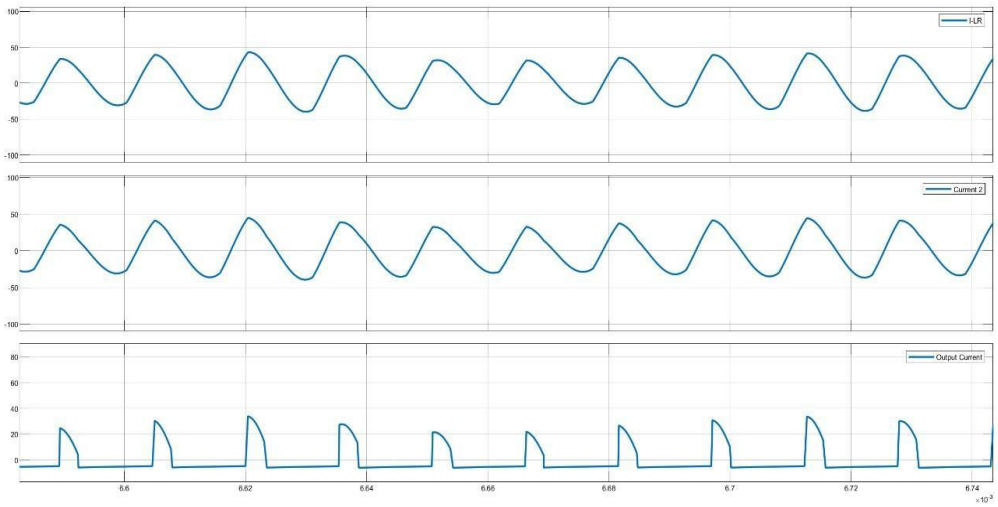


**Figure 19: Resonant current waveform in PWM 2 region**

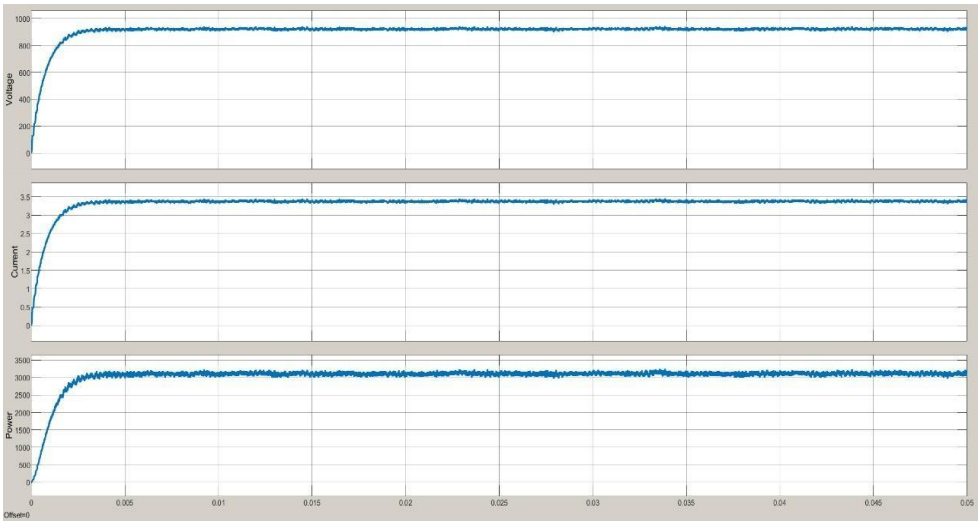


**Figure 20: Output Voltage, Power, Current Level in PWM 2 region**

## VII CONCLUSION

PWM-controlled SRC for EV chargers with a very wide range of gain. By adapting two PWM boost switches and a blocking capacitor with a full bridge rectifier, the configuration of the secondary side rectifier gradually converts from full bridge to voltage doubler as the output voltage increases. Thus, the proposed converter can achieve two peak efficiency points over the entire operating range. The proposed converter and control limits the efficiency drop of PWM control by limiting peak resonant current caused by boosting action, so the efficiency curve is high and flat over very wide output voltage range. Therefore, the proposed converter and control can be a strong candidate for the universal EV charger applications.

## REFERENCES

[1]. F. C. Lee, Q. Li, and A. Nabih, "High frequency resonant converters: An overview on the magnetic design and control methods," ***IEEE J. Emerg. Sel. Topics Power Electronics***, vol. 9, no. 1, pp. 11–23, Feb. 2021.

[2]. A. Mustafa and S. Mekhilef, "Dual phase LLC resonant converter with variable frequency zero circulating current phase-shift modulation for wide input voltage range applications," ***IEEE Trans. Power Electronics***, vol. 36, no. 3, pp. 2793–2807, Mar. 2021.

[3]. F. Musavi, M. Cracium, D. S. Gautam, and W. Everle, "Control strategies for wide output voltage range LLC resonant DC–DC converters in bat- tery chargers," ***IEEE Trans.*** Veh. Technol. vol. 63, no. 3, pp. 1117–1125, Mar. 2014.
[4]. J.-W. Kim, M.-Y. Park, J.-K. Han, M. Lee, and J.-S. Lai, "PWM resonant converter with asymmetric modulation for ZVS active voltage doubler rectifier and forced half resonance in PV application," ***IEEE Trans. Power Electron***. vol. 35, no. 1, pp. 508–521, Jan. 2020.
[5]. Dr. P S Bimbhra, "Power Electronics", Third Edition, Khanna Publishers Delhi, 2012.
[6]. Muhammad H Rashid, "Power Electronics Handbook: Devices, Circuits, and Applications", Second Edition, Academic Press.
[7]. L Umanand "Power Electronics Essentials and its Applications" Third Edition, Wiley Publishers.
[8]. Ved Mohan, Toren M Undeland, Willeam P Robbins"Power Electronics Converters, Applications and Design" Third Edition, Wiley Publishers.